Academic Sciences International Journal of Pharmacy and Pharmaceutical Sciences

ISSN- 0975-1491 Vol 5, Issue 4, 2013

Research Article

PREPARATION, *IN VITRO* AND *IN VIVO* EVALUATION OF ORAL INDOMETHACIN-HP-B-CYCLODEXTRIN LOADED CHITOSAN NANOPARTICLES

GINA S. EL-FEKY[a], SALLY T. EL-BANNA[b], SAFAA K. H. KHALIL[b]

[a]Department of Pharmaceutical Technology, Pharmaceutical Industries Division, National Research Center, Cairo, [b]Advanced Materials and Nanotechnology Group, Center of Excellence for Advanced Sciences (CEAS), Department of Spectroscopy, Division of Physics, National Research Center, Cairo, Egypt. Email: gelfeky@hotmail.com

Received: 12 Aug 2013, Revised and Accepted: 21 Sep 2013

ABSTRACT

The low solubility and the irritant effect of oral indomethacin (IND) on the lining of the stomach limit to a great extent its therapeutic potential. The aim of this study is first; to enhance the solubility of IND through complexation with hydroxyl propyl beta cyclodextrin (HP-β-CD) second, to incorporate the complex onto chitosan (CS) nanoparticles (NP), formed through ionic gelation, in order to control the drug release and to enhance its permeability and finally; to coat the complex loaded CS nanoparticles with alginate (ALG) to avoid drug release in the stomach and thus, reduce its gastrointestinal side effects. The solubility of IND increased linearly with increasing the HP-β-CD concentration indicating an A_L-type system. The 3:1 chitosan:tripolyphosphate (CS:TPP) ratio with 2mg/ml final CS concentration was capable of offering CS NP of 30nm with narrow particle size distribution and acceptable entrapment efficiency (41%). The alginate coated IND-HP-β-CD loaded CS NP was capable of providing a better oral delivery profile for IND where the cumulative release of IND in pH 1.2 was 0% then a total release amount of 68.97 was successfully delivered in pH 6.8. *In vivo* study on experimental animals showed a significantly high anti-inflammatory activity of ALG coated IND-HP-β-CD loaded CS NP containing 20 and 15 mg IND (F1 and F2, respectively) and a better analgesic activity compared to the market drug reference. F1 and F2 possessed gastroprotective property as was evidenced by their significant inhibition of the formation of gastric lesions normally induced by IND.

Keywords*:* Chitosan; HP-β-cyclodextrin; Nanoparticles; Oral; Indomethacin

INTRODUCTION

One of the most attractive areas of research in drug delivery today is the design of nanosystems that are able to deliver drugs to the right place, at appropriate time and at the right dosage. Nanoparticulate delivery systems have the potential power to improve drug stability, increase the duration of the therapeutic effect and permit both enteral and parenteral administration (1-3).

Indomethacin (IND), a gold standard non-steroidal anti-inflammatory drug (NSAID), is commonly used to reduce fever, pain, stiffness, and swelling. Inspite of being potent and highly effective, the drug shows many drawbacks (4).

The oral route is the most convenient and usually the safest and least expensive, however, it has general in addition to specific limitations when it comes to a drug like indomethacin (5). The low solubility in addition to the irritant and the harmful effect of oral indomethacin on the lining of the stomach limits to a great extent its therapeutic potential.

Cyclodextrins (CDs) are cyclic oligosaccharides consisting of six to eight glucose units linked by α-1,4-glucosidic bonds, resulting in the formation of toroidal molecules with internal hydrophobic cavities and external hydrophilic surface. Applications of CDs in oral drug delivery include improvement of drug bioavailability due to increased drug solubility, improvement of the rate and extent of dissolution, and/ or stability of the drug at the absorption site. In addition, CD complexation was found to decrease local drug irritation and also modify the time of drug release during GI transit (6,7). However, the unmodified CDs have cytotoxicity which limits their pharmaceutical applications. Various CDs derivatives have been developed to overcome these drawbacks, such as sulfobutylether β-cyclodextrin and hydroxypropyl β-cyclodextrin.

Recently, the idea of using nanoparticles made from natural biodegradable polymers to deliver drugs has provoked great interests. Among these, alginate (ALG) and chitosan (CS) have been widely exploited in the pharmaceutical industry for controlling drug release (8,9) and have received much attention for delivery of different therapeutic agents by intravenous, oral, and mucosal administration (10).

CS which is manufactured by partial deacetylation of chitin from crustacean shells (11) is a biodegradable and bioadhesive polysaccharide. It has been reported as nontoxic and soft tissue compatible in a range of toxicity tests (12, 13). Recently, CS was used in the application of peroral delivery of drugs (8), the addition of CS can not only endow nanoparticles positive surface charge, but also prolongs the time that the active ingredients contact with the epithelium and enhance absorption via the para-cellular transport pathway through the tight junctions (14, 15). Inspite of all its superior properties, chitosan has an apparent pKa of 5.6 and is highly soluble in acidic pH of the stomach which would make chitosan carrier lose its advantage in controlling the site and rate of release of the encapsulated indomethacin because of its hydrophilic nature and easy solubility in acidic medium. It might be an interesting method to overcome these obstacles by coating acid-resistant polymer, such as sodium alginate, onto the surface of chitosan nanoparticles.

Alginate (ALG) is a water soluble anionic polysaccharide extracted from brown seaweed and is composed of alternating blocks of 1-4 linked α-L-guluronic and β-Dmannuronic acid residues. ALG has been reported to be mucoadhesive, biodegradable, and biocompatible and has potential for numerous pharmaceutical and biomedical applications such as drug delivery system and cell encapsulation (16, 17). As an anionic polysaccharide, ALG can easily interact with cationic chitosan nanoparticles to form a polyelectrolyte complex coating via electrostatic interactions (18, 19). This ALG/CS polyelectrolyte complex provides a carrier system capable of protecting the drug in stomach media whereas, in intestinal pH they offer controlled release of the drug through the formed hydrogel matrix (3). ALG coated CS nanoparticles have been extensively investigated as polymeric carriers for a number of drugs (3, 20-22) however, the studies on the release of indomethacin from such carriers are limited.

The objective of this study is represented in enhancing the solubility and dissolution rate of indomethacin through complexation with HP-β-CD followed by complex incorporation onto chitosan nanoparticles in order to control the drug release and enhance its permeability and finally coating the CS nanoparticles with ALG to avoid drug release in the stomach thus reduce the indomethacin GI side effects.

MATERIALS AND METHODS

Materials

CS was purchased from Mallinckrodt, USA [M.W = 400000, degree of deacetylation 95%]. Tripolyphosphate was supplied by

Mallinckrodt, Netherland. Glacial acetic acid 99.8% was obtained from El Nasr Pharmaceutical Chemicals Co., Egypt. IND was purchased from Merck, USA. Pharmaceutical grade HP-β-CD was supplied by Roquette, France. Other chemicals and solvents were of analytical grade.

Preparation and characterization of IND-HP- β-CD complex

Phase solubility studies

Solubility study was carried out according to the method of Higuchi and Connors (6) and as was detailed in our previous work (23). An excess drug was added to distilled water containing different concentrations of HP-β-CD. The formed suspensions were shaken at 25 ± 0.5°C till equilibrium and then filtered through a millipore filter (0.45 µm). An aliquot portion of the filtrate was analyzed by a UV spectrophotometer (UV-240 1PC, Shimadzu, Japan) at λ_{max} 319.5 nm against a blank. The Experiment was performed in triplicate. The apparent stability constant ($K_{1:1}$) was calculated from the linear fit of the curve according to the following equation: $K_{1:1} = slope / D_0(1\text{-}slope)$

Where, Slope is the value found in the linear regression and D_0 is the intrinsic drug solubility derived from the intercept of the phase solubility relationship (24).

IND-HP-β-CD complexation

Physical mixture in addition to kneaded and coevaporated complexes were prepared in a 1:1 molar ratio of IND:HP-β-CD based on the results obtained from the phase solubility study.

Physical mixture was prepared by mixing the drug together with the HP-β-CD in a mortar for 10 min. **Kneaded complex** was prepared by adding water dropwise to IND-HP-β-CD mixture placed in a mortar until a homogeneous paste was formed. The resulting paste was then dried at 45 °C for 48 h and the solid was ground and finely sieved through a 250 µm sieve. **Co-evaporated complex** was prepared by dissolving equimolar amounts of HP-β-CD and IND in 250 ml of 50% aqueous ethanol. The solution was stirred till the complete dissolution of the mixed powders; the solvent was then evaporated at 45°C and reduced pressure using a rotary evaporator. The resulting solid was ground and sieved.

Characterization

Scanning Electron Microscopy (SEM)

Complexes were gold coated using a Hitachi coating unit IB-2 coater under a high vacuum, 0.1 Torr, high voltage, 1.2 kV and 50 mA. Coated samples were examined using SEM (JEOL JXA-840A SEM, Japan) to characterize the changes of both the drug and the HP-β-CD surfaces before and after complexation for indicating complex formation.

Fourier-Transform Infra Red (FTIR) spectroscopy

FTIR spectra of the complexes were obtained on a 6100 JASCO FTIR spectrometer, Japan. A 1% of each dried complex was mixed with KBr and compressed to form tablets. The IR spectra were scanned over the wave number range of 4000 to 400 cm^{-1} using a resolution of 4 cm^{-1} and 64 co-added scans.

Analysis of drug content in the IND-HP-β-CD complex

Drug content in the IND-HP-β-CD complex was determined by dissolving a specific amount of each complex in 10 ml ethyl alcohol and then measuring it spectrophotometrically at 319.5 nm.

Preparation and characterization of IND-HP-β-CD loaded CS nanoparticles

Preparation of IND-HP-β-CD loaded CS nanoparticles

CS solution was prepared dissolving a specific amount of CS in its equivalent amount of water. The pH of the CS solution was adjusted to 5.4 using 0.1N NaOH and a weighed amount of IND-HP-β-CD complex was then dissolved under magnetic stirring at 25±1C. After complete dissolution of IND complex, specific concentration of tripolyphosphate solution was then added dropwise to the IND-HP-β-CD/CS solution under continuous stirring. The resulting mixture was further sonicated.

Characterization of IND-HP-β-CD loaded CS nanoparticles

Particle size and Polydispersity index (PDI)

The mean particle size and polydispersity index (PDI) of IND-HP-β-CD loaded CS nanoparticles were determined using a photon correlation spectroscopy (Malvern Instruments, Worcestershire, United Kingdom), equipped with the Malvern PCS software (version 1. 27).

Entrapment efficiency IND-HP-β-CD loaded CS nanoparticles

The nanoparticles were separated from the aqueous dispersion medium by centrifugation at 9,000 rpm for 1 h. Entrapment efficiency (EE) was calculated according to the following equation (25).

$$EE\ (\%) = \frac{\text{Total amount of drug in the nanoparticles}}{\text{Initial amount of drug used for loading studies}} X100$$

Preparation of IND-HP-β-CD loaded CS NP powder

The aqueous suspension of the selected IND-HP-β-CD loaded CS NP formulation was spray dried using a laboratory-scale spray-dryer (Büchi® Mini Spray Dryer, B-290, Switzerland), under the following conditions; a feed rate of 2.5 ml/min, inlet and outlet temperatures of 120±2ºC and 85±2°C, respectively, an air flow rate and aspirator kept constant at 400 Nl/h and 80%, respectively in order to obtain dry powder (26).

Characterization of the selected IND-HP-β-CD loaded CS NP

FTIR spectroscopy (see under 2.2.3.2)

TEM

TEM was used to determine the size and morphology of prepared NP. One drop of the suspended NP was spread onto a carbon film 200 mesh copper grid and allowed to stand for 10 min. The samples were stained with one drop of 3% phosphotungestic acid before viewing under microscope (JEOL JEM-1230, Japan).

X-Ray Diffraction (XRD) Diffraction patterns of kneaded IND-HP-β-CD complex, blank CS NP and IND-HP-β-CD loaded CS NP were determined with an X-ray diffractometer (Empyrean, Pixcel^{3D}, Holland) at room temperature using a Cu Kα radiation (λ=1.54060 ^{0}A), a current of 30mA and voltage of 45kV. Fine powdered samples, were analyzed over the 5-80 2θ range with a scan step size of 0.0260 and time of acquisition of 18.8700 s.

Coating IND-HP-β-CD loaded CS NP with sodium alginate

Alginate (ALG) coated NP were obtained by mixing a specific amount of IND-HP-β-CD loaded CS NP and a distilled water solution of sodium alginate (1% w/v) under magnetic stirring. The agitation was maintained during a 20 min period. The suspension was then spray dried using (Büchi® Mini Spray Dryer, B-290, Switzerland) and the dry coated nanoparticles were collected.

Characterization of the ALG coated IND-HP-β-CD loaded CS NP

Zeta potential

The zeta potential of NP was measured using a Laser Zetasizer (Malvern Instruments model "Zetasizer 2000", UK) after dilution with double distilled water at ionic strength of $2x10^{-2}$ M NaCl.

***In vitro* release study**

Release of IND from its HP-β-CD complex alone as well as from the ALG coated and uncoated IND-HP-β-CD loaded CS NP were compared at 37±0.5oC using USP Dissolution Tester, Apparatus II. A specified amount of each preparation was immersed in 750 ml 0.1 N HCl (pH 1.2) equilibrated at 37±0.5°C and rotation rate of 50 rpm. Five ml aliquots of the medium were withdrawn at pre-set time intervals over 2 h and were replaced with 5 ml of fresh medium. The samples were filtered through 0.45 µm millipore filters and the amount of drug was

spectrophotometrically determined. After 2 h, 250 ml of 0.2 M tribasic sodium phosphate, pre-equilibrated at 37±0.5oC, were added to the dissolution vessel and the pH adjusted to pH 6.8, 5 ml samples were further withdrawn every hour for up to 24 hrs. IND content was measured spectrophotometrically at 319.5 nm. The percentage drug released and release profiles were determined.

***In-vivo* study**

All the animals involved in the in vivo experiments were provided by the National Research Center's animal house (Cairo, Egypt). All the animals were kept in a room under environmentally controlled conditions of 22±2°C and a 12h light–12h dark cycle. Animals had free access to standard diet and water before starting the experiments. The research was carried out according to the National Research Center's ethical protocol for the care and use of laboratory animals.

Acute Anti-inflammatory effect (Carrageenan-induced paw edema)

Twenty four female albino rats were used in the carrageenan-induced paw edema test (27, 28), these rats were randomly divided into 4 groups (n=6 in each group). Paw edema was induced by a sub-plantar injection of 100 µl of 1% carrageenan (lambda) in saline into the right hind paw of the rats. One hour before induction of edema, saline was administered orally to a group of animals that served as control (group 1). Drugs were administered as follows; Market IND (20 mg/kg) was administered orally to a group of rats that served as a positive control (group two), formula F1 (15 mg/kg) and formula F2 (20 mg/kg) of the ALG coated IND-HP-β-CD loaded CS NP were administered orally to group 3 and group 4, respectively. All the drugs were administered one hour before induction of inflammation. The right hind paw volume was measured immediately before carrageenan injection and at selected times (1, 2, 3 and 4 hours) thereafter using water plethysmometer. Anti-inflammatory activity was measured as the percentage reduction in edema level when drug was present, relative to control (29) as shown in Fig. 6.a.

Statistical analysis was carried out using repeated measures one way ANOVA followed by least significant test for multiple comparisons.

Anti-nociceptive (Analgesic) effect (Tail flick test)

Twenty four albino rats divided randomly into four equal groups were used in this study. Group 1 served as negative control, group 2 served as positive control where 20mg/kg of marketed indomethacin were administered to each rat. Groups 3 and 4 served as test groups where ALG coated IND-HP-β-CD loaded CS NP equivalent to 15mg/kg (F1) and 20 mg/kg of IND (F2) were administered to each group, respectively. All drugs were injected orally 30 minutes before placing the animal on the hot plate. Each animal was placed gently on the tail flick such that the tail is subjected to the IR beam. Latency to exhibit nociceptive responses, such as removing the tail was determined 30, 60, 90 min after administration of test substances or saline. Saline was administered subcutaneously (s.c.) to the control group. Values represent the mean ± S.E. Of six animals in each group.

Effect of IND formulations on the gastric ulcer number and severity

Albino rats, approximately of 150-200 g were used. They were divided into four groups of six animals each, the distribution of animals in groups were randomized. Group 1 served as negative control, group 2 served as positive control where 20mg/kg of market indomethacin were administered to each rat. Groups 3 and 4 served as test groups where 15mg/kg (F1) and 20 mg/kg (F2) of IND loaded NPs were administered to each group, respectively.

The stomach was removed, opened along the greater curvature, washed with saline and the inner surface was examined with a 6.4x binocular magnifier. Lesions were assessed visually. Gastric lesions were evaluated according to their number and severity (scored between 0; no visible ulcers, and 10; deep lesion with a diameter greater than 10 mm), in each stomach. The scores for each single lesion were then totaled (30). Each value represents the mean of 6 rats ± SE. Statistical analysis was carried out using Kruskal-Wallis non parametric one way ANOVA.

RESULTS AND DISCUSSION

IND-HP-β-CD complex formation

Phase solubility study

The phase solubility study represents a basic requirement for optimizing the inclusion complex and evaluating the affinity of a certain drug to a specific CD. This process has been widely used to determine the molar ratio at which the drug forms a complex with CD.

The solubility of IND increased linearly with increasing the concentration of HP-β-CD in water as shown in fig. 1 which indicates that the phase solubility curve represents an A_L-type system (6). The slope value was less than one which refers to an inclusion complex in the molar ratio of 1:1 (IND: HP-β-CD) molecules (31, 32). The solubilizing power of HP-β-CD towards IND was found to be 0.79925 x10^{-3} mM and the apparent stability constant, $K_{1:1}$, was found to be 170.08 M^{-1}. Therefore, it can be concluded that a stable inclusion complexes between IND and HP-β-CD in 1:1 molar ratio was formed (33).

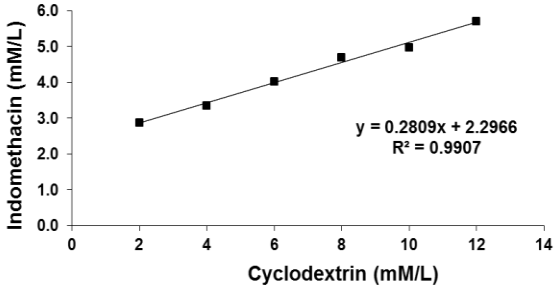

Fig. 1: Phase solubility diagram

Preparation and characterization of IND-HP-β-CD complex

IND-HP-β-CD binary mixtures were prepared using physical mixing as well as kneading and coaevaporation processes. The prepared systems were further characterized to assess complex formation.

SEM

Micrographs of HP-β-CD, IND and binary mixtures are shown in fig. 2a-2e. HP-β-CD consisted of regularly shaped crystals (fig. 2a) and IND was demonstrated as large aggregates of small particles (fig. 2b). IND-HP-β-CD physical mixture appeared as agglomerated particles of IND adhered on the crystal surfaces of HP-β–CD (fig. 2c). In the kneaded and the coevaporated complexes, the original morphology of the raw materials disappeared and separating the IND from the HP-β-CD was not possible, suggesting complex formation (33). The kneaded complex appeared as bulky non-porous particles (fig. 2d), whereas, in the coevaporated complex, medium sized agglomerates randomly arranged (fig. 2e).

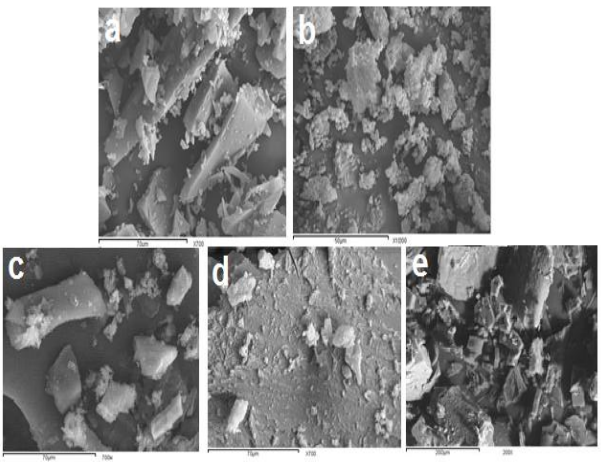

Fig. 2 SEM of HP-β-CD (a), IND (b), Physical mixture (c), kneaded complex (d) and coevaporated complex (e)

FTIR spectroscopy

Scanning IND, two absorbance peaks at 1715 and 1690 cm^{-1}; corresponding to carbonyl & benzoyl stretching (C=O), respectively (34-36); were reported in the physical and kneaded mixtures. In the co-evaporated mixture, the peaks at 1715 and 1690 cm^{-1} were shifted to much lower frequencies at 1687 and 1606 cm^{-1}, respectively (fig. 3). This finding supports the hypothesis that IND molecules have suffered a chemical change during the coevaporation complexation process. In addition, The prominent absorbance peaks of HP-β-CD at 3400 cm^{-1} (O-H), 2930 cm^{-1} (C-H), 1157 cm^{-1} (C-H), 1085 cm^{-1} (C-O) for stretching vibrations, 1655 cm^{-1} (H-O-H)) for bending vibrations and 1030 cm^{-1} (C-O-C) (37, 38) were observed in all prepared IND-HP-β-CD complexes (fig. 3) indicating the presence of a host-guest interaction and confirming complex formation.

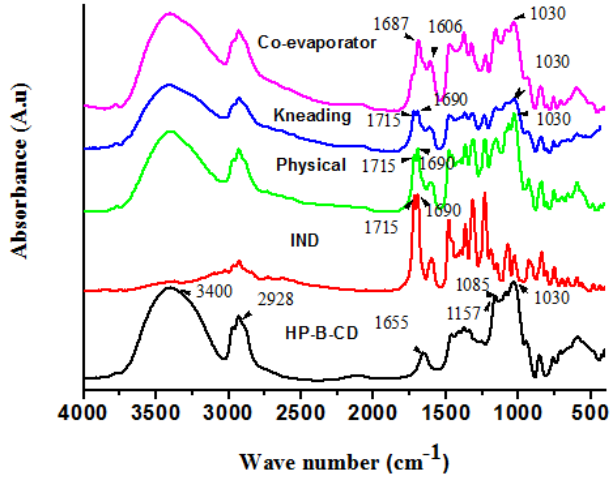

Fig. 3: FTIR of HP-β-CD, IND and formed complexes

IND content in the IND-HP-β-CD complex

Comparing the theoretical drug content in the IND-HP-β-CD prepared complexes to their actual drug content, the physical mixture showed an excellent agreement (31.5 mg *vs.* 35mg, respectively), the kneaded mixture showed a good agreement (31.5 mg vs. 22.97 mg), whereas, the coevaporated mixture showed a poor agreement (31.5 mg vs. 8.98 mg, respectively) which might be attributed to the severe chemical changes the IND molecule suffered from during the coevaporation process as indicated by the FTIR results. Therefore, due to its ability of complex formation in addition to its reasonable drug content, the kneading method was used for preparing IND- HP-β-CD complex.

Preparation and characterization of IND- HP-β-CD loaded chitosan nanoparticles

Preparation of IND-HP-β-CD loaded chitosan nanoparticles with different CS:TPP weight ratios

IND-HP-β-CD-loaded CS nanoparticles were prepared using a two-step procedure based on the formation of IND-HP-β-CD complex first (as discussed above) followed by ionotropic gelation of CS with TPP [39]. There are several factors that may affect the properties of IND-HP-β-CD loaded CS nanoparticles. One main factor is the concentration of CS because the production of CS gel is a key step of this process. If the concentration of CS is too low, the gel will be of poor quality. On the contrary, a high concentration of CS will lead to the formation of a continuous gel (40). A second important factor that could affect the EE and size of the formed nanoparticles is the w/w ratio of CS:TPP, as it determines the quantity of stabilizing polyanion needed to entrap the maximum amount of IND during formulation. Therefore, IND-HP-β-CD loaded CS nanoparticles were prepared using different CS:TPP weight ratios from 1:1 and up to 6:1. The stirring speed could also affect the EE and nanoparticle size, which will finally lead to different drug release profiles. After a series of experiments (data not shown), the stirring speed was adjusted to 600 rpm.

Characterization of IND- HP-β-CD loaded CS nanoparticles prepared with different CS:TPP weight ratios

Particle size and polydispersity index

The mean diameter of IND-HP-β-CD-loaded CS nanoparticles prepared with CS:TPP weight ratios of 1:1 up to 3:1 increased from 10 up to 30 nm with a PDI ranging from 0.149 up to 0.264, further increase in the CS:TPP ratio led to a subsequent reduction in the particle diameter reaching a 10 nm with the ratio 6:1. It's worth noting that increasing the CS:TPP ratio was accompanied by an increase in the PDI values to 0.350 indicating lower uniformity in the particle size distribution at higher ratios.

The above findings could be explained as follows, first, it seems that HP-β-CD exerts a significant influence on the particle size as all the loaded systems were generally of a markedly small size, which may be because of the electrostatic attraction that can condense the nanoparticle into a more compact system (40). Second, as was mentioned in our previous work (23) the decrease in the particle size accompanying the increase in the CS:TPP ratio might be mainly due to a reduction in ionic bond formation (39) indicating that the 3:1 CS:TPP ratio might offer a stoichiometric proportion of the functional groups of both polymers which consequently results in optimum particle size and PDI.

Entrapment efficiency of CS nanoparticles

EE of IND-HP-β-CD loaded chitosan nanoparticles was found to be somewhat higher with high CS:TPP weight ratios (3:1; 41%) compared to lower weight ratios (2:1 and 1:1; 25% & 23%, respectively). Lower chitosan concentrations might have lead to aggregation of nanoparticles due to the minimized electrostatic repulsion between them. Further increase in the CS: TPP weight ratio up to 6:1, didn't have any significant effect on the EE.

The IND-HP-β-CD complexation process might have greatly promoted the encapsulation of the hydrophobic IND molecules into the hydrophilic CS nanoparticles due to the electrostatic attractions among HP-β-CD, IND and the CS shell (40).

The effect of changing the CS final concentration (0.5, 1, 1.5, 2, 2.5 and 3 mg/ml) was investigated within the CS:TPP ratio 3:1 as it was capable of providing CS nanoparticles with acceptable size, uniform particle size distribution and high EE.

Characterization of IND- HP-β-CD loaded CS nanoparticles prepared with different CS concentrations within the 3:1 CS:TPP weight ratio

Particle size and polydispersity index

Increasing the CS concentration from 0.5 up to 2 mg/ml within the 3:1 CS:TPP weight ratio, no general trend concerning the particle size of the prepared IND- HP-β-CD loaded CS nanoparticles was observed. However, the nanoparticles showed a significantly larger diameter with increasing the chitosan concentration over 2 mg/ml (405 and 596 for 2.5mg/ml and 3mg/ml, respectively).

The lowest particle diameter together with the highest uniformity in the particle size distribution, as indicated by PDI values, were observed with CS concentration of 2 mg/ml (30 nm and 0.149, respectively), data not shown.

Entrapment efficiency

EE was gradually increased from 20% up to 41% with increasing CS final concentration from 0.5 mg/ml up to 2 mg/ml, respectively, further increase in CS concentration led to a gradual decrease in the EE reaching 20 % with 3 mg/ml final CS concentration.

This could be simply explained on the basis of the variability in the viscosity of CS with its different tested concentrations. At low CS concentrations (from 0.5 to 1 mg/ml), the viscosity might have been too low to promote the gelation between CS and TPP and in turn to promote the entrapment of IND, increasing the concentration to 2mg/ml might have offered ideal viscosity and thus, showed maximum gelation and subsequently, maximum IND entrapment, further increase in CS concentration to 3 mg/ml, the

viscosity of the gelation medium highly increased hindering the drug entrapment (23).

The above findings demonstrated that the 3:1 CS:TPP ratio with 2mg/ml final CS concentration could offer small sized CS nanoparticles (30 nm) with narrow particle size distribution (PDI=0.149) and acceptable EE (41%) (23).

Therefore, it is to be noted that the NP formulation prepared at the CS:TPP weight ratio of 3:1 using 2 mg/ml final CS concentration will be a subject of further investigations using TEM, FTIR, XRD. This specific formulation will subsequently be coated with sodium alginate (ALG) in an attempt to delay the release process within the stomach and in turn overcome the pH sensitivity limitation of CS and reduce IND side effects on the stomach and will be characterized for its Zeta-potential, *in vitro* release profile and *in vivo* effect.

Characterization of the selected IND-HP-β-CD loaded CS nanoparticle

TEM

TEM image (fig. 4a) demonstrated the IND-HP-β-CD loaded CS NP as spherical dispersed particles with size range of 50–100 nm. Encapsulation of IND- HP-β-CD onto the CS NPs was also confirmed.

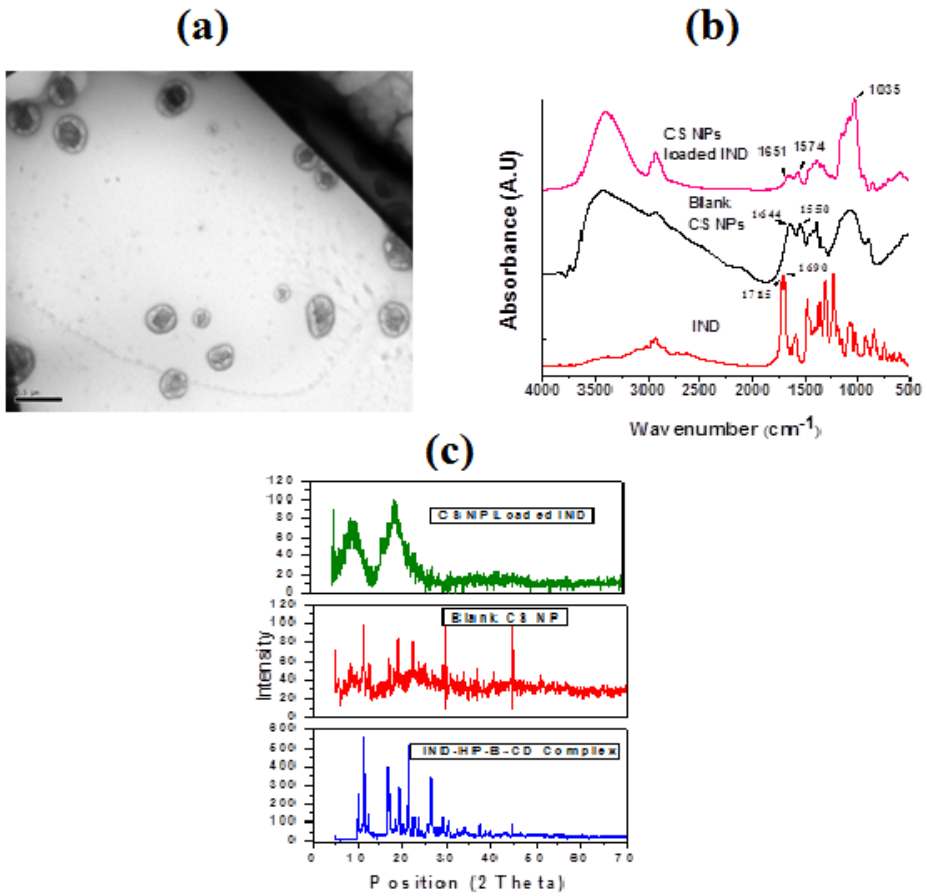

Fig. 4a: TEM of HP-β-CD-IND loaded CS NP, 4b FTIR of HP-β-CD-IND loaded CS NP, 4c XRD of HP-β-CD-IND loaded CS NP

FTIR

Comparing FTIR spectra of the selected IND-HP-β-CD loaded CS NP to that of the blank CS NP (fig. 4b), spectral changes resulting from IND encapsulation were reported, basically, the C=O amid I peak at 1644 cm^{-1} of the blank CS NP was shifted to 1651 cm^{-1} with a markedly lower intensity. Again comparing the FTIR spectra of IND to encapsulated IND, the major characteristic peaks of IND; 1715 cm^{-1} acidic (C=O) and 1690 cm^{-1} ketonic (C=O) were found to disappear except for the peak at 1035 cm^{-1} (C-O) which remained unchanged. FTIR changes confirmed the strong interaction between the C=O group of IND and the NH_2 group of CS/TPP matrix resulting from drug loadings (25, 41, 42)

XRD

Assessing the XRD diffraction pattern of the kneaded IND-HP-β-CD binary mixture, the blank CS NP and the IND-HP-β-CD loaded CS NP (fig. 4c), the kneaded complex presented several peaks implying their crystalline nature, while the blank CS NP showed some major peaks at approximately 11^0, 19^0, 22.5^0, 29^0, 44.5^0 and 72.5^0 with strongest intensity at $2\theta = 44.5^0$. The diffraction pattern of IND-HP-β-CD loaded CS NP provoked two broad peaks at $2\theta = 9.3^0$ and 19^0 with no characteristic peaks of the crystalline drug which supports the formation of the IND-HP-β-CD complex (37).

Preparation and characterization of ALG coated IND-HP-β-CD loaded CS NP

Preparation of ALG coated IND-HP-β-CD loaded CS NP

As we previously discussed, pH value of gastric fluid is approximately 2 which will enhance the solubility of CS after the oral administration with subsequent uncontrolled release of IND in the stomach. Therefore, it became very important to develop a carrier based on CS and ALG in order to effectively avoid the acidic degradation of CS and in turn limit the gastric side effects of the encapsulated IND. Here, ALG coating of the selected CS nanoformulation followed by characterization and comparative analysis between uncoated and ALG coated CS NP were carried out. Coating of ALG onto CS NP could improve its stability and modify the release behavior of IND.

Characterization of ALG coated IND-HP-β-CD loaded CS NP

Zeta potential

The zeta potential of the selected blank NP was found to be 32.4 mV, which decreased to 11.3 mV after IND incorporation. This might be due to the high charge density of IND which at neutral pH might have deprotonated most of the amino groups of CS (43). However, the zeta potential of the ALG coated IND-HP-β-CD loaded CS NP was found to be 44.3mV which means that ALG coated CS NP could provide an effective protection to IND-HP-β-CD due to the strong electrostatic attraction and thus, acceptable stability can be predicted for the prepared nano formulation (44).

Results indicated that the prepared coated NP have good stability compared the uncoated one (25).

***In vitro* release study**

To investigate the capability of the designed system to deliver IND orally in the intestine, the cumulative release profiles of IND from the initially formed IND-HP-β-CD 1:1 kneaded complex, uncoated IND-HP-β-CD loaded CS NP and the ALG coated IND-HP-β-CD loaded CS NP were compared in pH 1.2 for 2 hr followed by 4 hr in pH 6.8 (fig. 5).

Considering the IND-HP-β-CD kneaded complex, a gradual constant zero order release profile was achieved with a 27.98% of the drug released 5 hrs after starting the experiment. In the uncoated IND-HP-β-CD loaded CS NP, IND was released in a burst effect in pH 1.2 in the initial 2 hr, as a result 64.16% of the encapsulated IND was released before reaching the intestine and only11% of the loaded IND were released in pH 6.8 in the following 3 hr. This result is in agreement with a number of previous studies (15, 40).

On the other hand, the ALG coated IND-HP-β-CD loaded CS NP exhibited a much better oral delivery profile for IND (fig 5); the cumulative release of IND in pH 1.2 was 0% then a total release amount of 68.97 was successfully delivered in pH 6.8. The coated drug loaded CS NP was able to offer a full drug protection in pH 1.2 followed by controlled release of IND in pH 6.8. This could be explained as follows; the cationic polymer (HP-β-CD) forms a compact complex with IND by both electrostatic attraction and inclusion, IND is thus retained in the core of the CS NP in the form of IND-HP-β-CD complex. Coating the CS NP with ALG offers an efficient protection for IND due to the electrostatic attraction between the positive amino groups of CS and the negative carboxylic groups of ALG. This attraction force prevents the NP from being dissolved in acidic pH. When the NP is transported to pH 6.8, 40% of the encapsulated drug were released initially in half an hour followed by a more gradual rate (15). The release mechanism is mainly a combination of both diffusion and erosion (45) where the rapid hydration of the alginate and then CS results in swelling of the carrier with subsequent fast drug release by diffusion then erosion of the polymer starts to take place gradually.

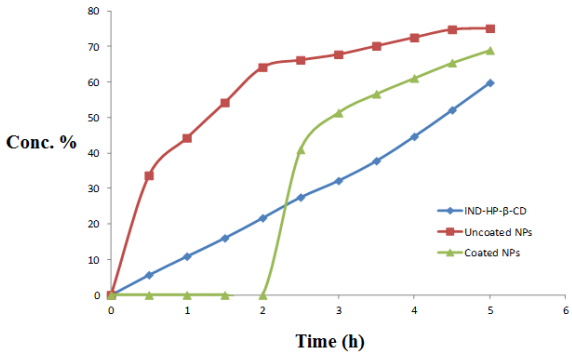

Fig. 5: *In vitro* release profile of IND from prepared systems

***In vivo* study**

Acute Anti-inflammatory effect (Carrageenan-induced paw edema)

Carrageenan-induced rat paw oedema is used widely as a working model of inflammation in the search for new anti-inflammatory drugs. The anti-inflammatory activity of the nanoformulations F1 (containing 15 mg IND) and F2 (containing 20 mg IND) *vs* a control as well as an IND market product was evaluated by carrageenan-induced rat paw oedema method [27, 28] and the results are compared in fig. 6a.

The results showed that F2; ALG coated IND-HP-β-CD loaded CS NP with a dose of 20 mg IND; showed minimum percentage change in the paw oedema volume among all tested formulations reaching only 15.51±3.2% increase in the oedema volume 4 hours after drug administration.

This result indicated that F2 with a dose of 20 mg IND showed a maximum anti-inflammatory activity as compared to the market product, which showed 47.29±3.6 % increase in the oedema volume after 4 hours, results are statistically significant (P<0.05). F1 with a dose 15 mg IND showed 18.05±1.4 % increase in the volume of paw oedema which is also significantly low as compared to the reference drug (P<0.05).

Significantly high anti-inflammatory activity of F1 (20 mg IND) and F2 (15 mg IND) indicates the efficacy of the developed nanocarrier in enhancing the therapeutic action of IND in acute anti-inflammatory conditions.

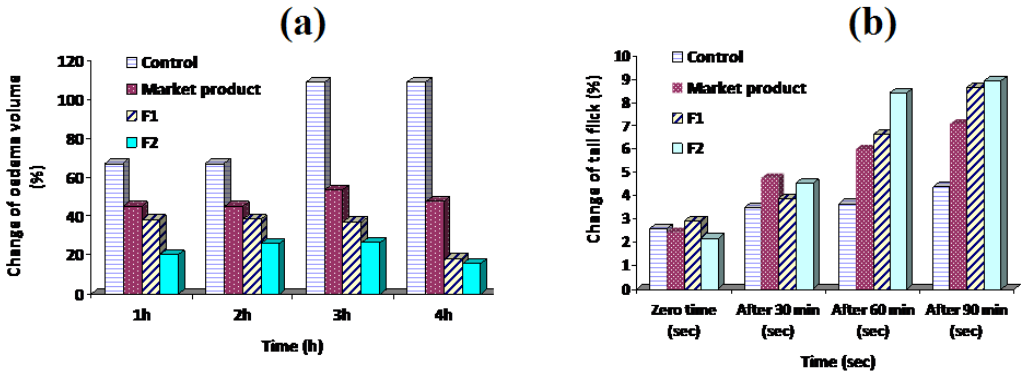

Fig. 6a *In vivo* anti-inflammatory effect of ALG coated HP-β-CD-IND loaded CS NP, 6b *In vivo* analgesic effect of ALG coated HP-β-CD-IND loaded CS NP

Anti-nociceptive (Analgesic) effect (Tail flick test)

The tail flick test measures the complex response to a non-inflammatory and acute nociceptive input. Results of the tail flick test are presented in (fig. 6b)

Both nanoformulations F1 (15 mg IND) and F2 (20 mg IND) were found to exhibit a dose dependent increase in the latency time compared to each other. Compared to the control and market product groups, they showed a higher latency time 90 minutes from

baseline. At 90 minutes, the latency time was 8.92±0.86 sec and 8.65±0.63 sec for F2 and F1, respectively compared to7.1±0.57 sec and 4.37±0.25 sec for the market product and the control group, respectively.

Therefore, it could be assumed that F1 and F2 might be capable of offering a better analgesic activity compared to the market drug reference.

Effect of IND formulations on the gastric ulcer number and severity

Administration of IND market product resulted in the production of gastric mucosal damage mainly in the glandular segment of the stomach. While, treatment of the animals with IND loaded nanoformulations (F1 and F2) was effective in totally eliminating ulceration in a dose-independent manner.

The results of this study demonstrated that the ALG coated IND-HP-β-CD loaded CS NP formulations (F1 and F2) possess gastroprotective property as evidenced by their significant inhibition of the formation of gastric lesions normally induced by IND.

CONCLUSION

The solubility of IND increased with HP-β-CD complexation. The 3:1 chitosan:tripolyphosphate (CS:TPP) ratio with 2mg/ml final CS concentration offered CS NP of 30 nm with narrow particle size distribution and acceptable entrapment efficiency (41%). ALG coated IND-HP-β-CD loaded CS NP was capable of providing a better oral delivery profile for IND where the cumulative release of IND in pH 1.2 was 0% then a total release amount of 68.97 was successfully delivered in pH 6.8. *In vivo* study on experimental animals showed ALG coated IND-HP-β-CD loaded CS NP, containing 20 and 15 mg IND, having a more effective anti-inflammatory and analgesic activities compared to a market drug reference and at the same time possessing a gastroprotective property.

REFERENCES

1. Florence, A.: The oral absorption of micro- and nanoparticulates: Neither exceptional nor unusual. Pharm. Res. 14, 259–266 (1997).
2. De, S., Robinson, D.: Polymer relationships during preparation of chitosan–alginate and poly-L-lysine–alginate nanospheres. J. Control Rel. 89, 101–112 (2003).
3. Sarmento, B., Ribeiro, A. J., Veiga, F., Ferreira, D. C., Neufeld, R. J.: Insulin-loaded nanoparticles are prepared by alginate ionotropic pre-gelation followed by chitosan polyelectrolyte complexation. J. Nanosci. Nanotechnol. 7, 2833–2841 (2007a).
4. Dillon, C. T., Hambley, T. W., Kennedy, B. J., Lay, P. A., Zhou, Q. D., Davies, N. M., *et al*.: Gastrointestinal toxicity, anti-inflammatory activity, and superoxide dismutase activity of copper and zinc complexes of the antiinflammatory drug indomethacin. Chem. Res. Toxicol. 16, 28–37 (2003).
5. Kagan, V. E., Tyurina, Y. Y., Tyurin, V. A., Konduru, N. V., Potapovich, A. I., Osipov, A. N., Kisin, E. R., Schwegler-Berry, D., Mercer, R., Castranova, V., Shvedova, A. A.: Direct and indirect effects of single walled carbon nanotubes on RAW 264.7 macrophages: role of iron. Toxicol. Lett. 165, 88-100 (2006).
6. Higuchi, T., & Connors, K. A.: Phase-solubility techniques. Adva. Anal. Chem. Instr. 4, 212-217 (1965).
7. Stella, V. J., Rajeswski, R. A.: Cyclodextrins: their future in drug formulation and delivery. Pharm. Res.14, 556-567 (1997).
8. Murata, Y., Jinno, D., Liu, D., Isobe, T., *et al*.: The drug release profile from calcium-induced alginate gel beads coated with an alginate hydrolysate. Molecules. 12, 2559–2566 (2007).
9. Shi, J., Alves, N. M., Mano, J. F.: Chitosan coated alginate beads containing poly(N-isopropylacrylamide) for dual-stimuli-responsive drug release. J. Biomed. Mater Res. B. Appl. Biomater. 84, 595–603 (2008).
10. Janes, K. A., Calvo, P., Alonso, M. J.: Polysaccharide colloidal particles as delivery systems for macromolecules. Adv. Drug Deliv. Rev. 47, 83-97 (2001).
11. Kristl, J., Smid-Korbar, J., Strue, E., Schara, M., Rupprecht, H.: Hydrocolloids and gels of chitosan as drug carriers. Int. J. Pharm. 99, 13-9 (1993).
12. Arai, K., Kinumaki, T., Fujita, T.: Toxicity of chitosan. Tokai. Reg. Fish Lab. 43, 89-94 (1968).
13. Nicol, S. *et al.*: Life after death for empty shells. New Scientist. 129, 46-8 (1991).
14. Kotze, A. F., Thanou, M. M., Luebetaen, H. L., de Boer, A. G., *et al*.: Enhancement of paracellular drug transport with highly quaternized N-trimethyl chitosan chloride in neutral environments: In vitro evaluation in intestinal epithelial cells (Caco-2). J. Pharm. Sci. 88, 253–257 (1999).
15. Sarmento, B., Ferreira, D. C., Jorgensen, L., van de Weert, M.: Probing insulin's secondary structure after entrapment into alginate/chitosan nanoparticles. Eur. J. Pharm. Biopharm. 65, 10–17 (2007b).
16. Smidsrod, O., Skjakbraek, G.: Alginate as immobilization matrix for Cells. Trends Biotechnol. 8, 71–78 (1990).
17. Gombotz, W. R., Wee, S. F.: Protein release from alginate matrices. Adv. Drug. Deliv. Rev. 31: 267–285 (1998).
18. Chen, Y., Siddalingappa, B., Chan, P. H. H., Benson, H. A. E.: Development of a chitosan-based nanoparticle formulation for delivery of a hydrophilic hexapeptide, dalargin. Biopolymers 90, 663–670 (2008).
19. Liouni, M., Drichoutis, P., Nerantiz, T. E.: Studies of the mechanical properties and the fermentation behavior of double layer alginate-chitosan beads, using Saccharomyces cerevisiae entrapped cells. World Journal of Microbiology and Biotechnology. 24, 281-288 (2008).
20. De Campos, A. M., Sánchez, A., Alonso, M. J.: Chitosan nanoparticles: a new vehicle for the improvement of the delivery of drugs to the ocular surface. Application to cyclosporin A. Int. J. Pharm. 224, 159–168 (2001).
21. Xu, Y. M., Du, Y. M.: Effect of molecular structure of chitosan on protein delivery properties of chitosan nanoparticles. Int. J. Pharm. 250, 215–226 (2003).
22. Douglas, K. L., Tabrizian, M.: Effect of experimental parameters on the formation of alginate–chitosan nanoparticles and evaluation of their potential application as DNA carrier. J. Biomater Sci. Polymer Edn.16, 43–56 (2005).
23. Khalil, H. K. S., El-Feky, S. G., El-Banna, T. S., and Khalil, A. W.: Preparation and evaluation of warfarin-β-cyclodextrin loaded chitosan nanoparticles for transdermal delivery. Carbohydrate Polymers. 90, 1244– 1253 (2012).
24. Marcus, E., Brewster, M. E., & Loftsson, T.: Cyclodextrins as pharmaceutical solubilizers. Advanced Drug Delivery Reviews. 59, 645–666 (2007).
25. Anitha, A., Maya, S., Deepa, N., Chennazhi, K. P., Nair, S. V., & Tamura, H.: Efficient water-soluble biodegradable polymeric nanocarrier for the delivery of curcumin to cancer cells. Carbohydrate Polymers. 83, 452–461 (2011).
26. Grenha, A., Remunan-Lopez, C., Carvalho, E. L., & Seijo, B.: Microspheres containing lipid/chitosan nanoparticles complexes for pulmonary delivery of therapeutic proteins. Eur. J. Pharm. Biopharm. 69, 83-93 (2008).
27. Winter, C. A., Risley, E. A., and Nuss, G. W.: Carrageenan induced edema in hind paw of the rat as an assay for anti-inflammatory drugs. Proc. Soc. Exp. Biol. Med. 111, 544-547 (1962).
28. Adeyemi, O. O., Okpo, S. O., Ogunti, O. O.: Analgesic and anti-inflammatory effect of the aqueous extract of leaves of Persea americana Mill (Lauraceae). Fitoterapia. 73, 375-380 (2002).
29. Duffy, J. C., Dearden, J. C., Rostron, C.: Design, Synthesis and biological testing of a novel series of anti- inflammatory drugs. J. Pharm. Pharmacol. 53, 1505-1514 (2001).
30. Valcavi, U., Caponi, R., Brambilla, A., Palmira, F., and Fuwagali, R.: Gastric anti-secretory, anti-ulcer and cytoprotective properties 9-hydroxy-19, 20-bis-nor-prostanoic acid in experimental animals. Arzneim. Forsch. 32, 657-663 (1982).
31. Casella, R., Williams, D., Jambhekar, S.: Solid-state β-cyclodextrin complexes containing indomethacin, ammonia, and water. I. Formation studies. Int. J. Pharm. 165, 1–14 (1998a).
32. Jambhekar, S., Casella, R., Mahera, T.: The physicochemical characteristics and bioavailability of indomethacin from β-cyclodextrin, hydroxyethyl-β-cyclodextrin, and hydroxypropyl-β-cyclodextrin complexes. Int. J. Pharm. 270, 149-66 (2004).
33. Onyeji, C. O., Omoruyi, S. I., Oladimeji, F. A., Soyinka, J. O.: Physicochemical characterization and dissolution properties of

binary systems of pyrimethamine and 2-hydroxypropyl-β-cyclodextrin. Afr. J. Biotechnol. 8, 1651–1659 (2009).

34. Taylor, L. S., Zografi, G.: Spectroscopic characterization of interactions between PVP and indomethacin in amorphous molecular dispersions. Pharm. Res. 14, 1691–1698 (1997).
35. Bandia, N., Weib, W., Robertsc, C. B., Kotrac, L. B., Kompellaa, B. U.: Preparation of budesonide– and indomethacin–hydroxypropyl-β-cyclodextrin (HPBCD) complexes using a single-step, organic-solvent-free supercritical fluid process. European Journal of Pharmaceutical Sciences. 23, 159-168 (2004).
36. Rezaei, M. A., Kebriaee, Z. A., Keshavarz, M., Ahmadi, A., Mohtat, B.: Preparation and in-vitro evaluation of indomethacin nanoparticles. Daru. J. Pharmceut. Sci. 18, 185-192 (2010).
37. Jun, S. W., Kim, M. S., Kim, J. S., Park, H. J., Lee, S., Woo, J.S., Hwang, S. J.: Preparation and characterization of simvastatin/hydroxypropyl-β-cyclodextrin inclusion complex using supercritical antisolvent (SAS) process. European Journal of Pharmaceutics and Biopharmaceutics. 66, 413-421 (2007).
38. Pankaj, G., Patil, C., Kalyane, N., Pore, N.: Effect of Hydrophilic Polymers on PioglitazoneI Complexation With Hydroxypropyl-β -Cyclodextrin. Digest Journal of Nanomaterials and Biostructures. 4, 891 – 897 (2009).
39. Calvo, P., Remunan-Lopez, C., Vila-Jato, J. L., & Alonso, M. J.: Chitosan and chitosan/ethylene oxide-propylene oxide block copolymer nanoparticles as novel carriers for proteins and vaccines. Pharm Res. 14, 1431-1436 (1997).
40. Zhang, N., Li, J., Jiang, W., Ren, C., Li, J., Xin, J., and Li, k.: Effective protection and controlled release of insulin by cationic β-cyclodextrin polymers from alginate/chitosan nanoparticles. International Journal of Pharmaceutics. 393, 212–218 (2010).
41. Chen, Y., Mohanraj, V. J., & Parkin, J. E.: Chitosan-dextran sulfate nanoparticles for delivery of an antiangiogenesis peptide. Int. J. Peptide Res. Ther. 10, 621–629 (2003).
42. Papadimitriou, S., Bikiaris, D., Avgoustakis, K., Karavas, E., & Georgarakis, M.: Chitosan nanoparticles loaded with dorzolamide and pramipexole. Carbohydrate Polymers. 73, 44-54 (2008).
43. Tang, D. W., Yu, S. H., Ho, Y. C., Mi, F. L., Kuo, P. L., & Sung, H. W.: Heparinized chitosan/poly(g-glutamic acid) nanoparticles for multi-functional delivery of fibroblast growth factor and heparin. Biomaterials. 31, 9320-9332 (2010).
44. Naghibzadeh, M., Amani, A., Amini, M., Esmaeilzadeh, M., Mottaghi-Dastjerdi, N., and Faramarzi, M., A.: An Insight into the Interactions between α-Tocopherol and Chitosan in Ultrasound-Prepared Nanoparticles. ,Journal of Nanomaterials. 2010, 1-7 (2010).
45. Arora, S., Gupta, S., Narang, K. R., Budhiraja, D. R.: Amoxicillin Loaded Chitosan-Alginate Polyelectrolyte Complex Nanoparticles as Mucopenetrating Delivery System for H. Pylori. Sci. Pharm. 79, 673–694 (2011).